Sliding Friction with Polymer Brushes

Rafael Tadmor,* Joanna Janik,† and Jacob Klein‡

Department of Materials and Interfaces, Weizmann Institute of Science, Rehovot 76100, Israel and Physical and Theoretical Chemistry Laboratory, South Parks Road, Oxford OX1 3QZ, United Kingdom

Lewis J. Fetters§

Exxon Research and Engineering Corporation, Annandale, New Jersey 08801, USA

(Received 2 May 2002; published 9 September 2003)

Using high-resolution shear force measurements, we examine in detail the frictional drag between rubbing surfaces bearing end-tethered polymeric surfactants (brushes). The drag attains a maximum on initial motion, attributed to elastic stretching of the chains, which falls by a cascade of relaxations to a value characteristic of kinetic friction. This has a very weak velocity dependence, attributed to chain moieties dragging within a self-regulating, mutual interpenetration zone. When sliding stops, the shear stress across the polymer layers decays logarithmically with time, consistent with the relaxation of a network of dangling ends.

DOI: 10.1103/PhysRevLett.91.115503 PACS numbers: 81.40.Pq, 79.60.Dp, 83.10.Gr

Rubbing of polymer-coated surfaces is implicated in phenomena ranging from biolubrication [1] to hard disk drives [2]. Polymer brushes have, in particular, been extensively researched [3], including their adhesion [4] and friction modification at polymer surfaces by end-tethered chains [5]. The molecular mechanism of friction between compressed brushes, however, is difficult to access experimentally, and despite much investigation [3,7–10] is still poorly understood. Earlier studies [8,11] were stymied by the onset of glassy behavior of the chains on strong compression and could shed little light on the detailed mechanism of frictional dissipation. Using a newly developed surface force balance (SFB) [12], together with a low glass-transition temperature (T_g) polymer, we studied the frictional drag between sliding polymer brushes. A maximum in the frictional force on initial sliding motion, attributed to stretching of the interpenetrated chains, falls via a cascade of relaxations to a characteristic kinetic friction. This depends only very weakly on the sliding velocity, an effect attributed to a velocity-dependent interpenetration of the opposing polymer layers. When the sliding motion ceases, the residual shear stress decays logarithmically with time, at a rate consistent with the relaxation of an entangled network of dangling ends.

The SFB used is capable of measuring normal and, in particular, extremely small shear stresses between sliding surfaces [12]. We used the low-T_g polymer poly(ethylene-propylene), (PEP : -$[CH_2$-CH_2-$CH(CH_3)CH_2]_N$-), end-functionalized with a zwitterionic group [13] to form brushes on mica surfaces by spontaneous assembly from solution (Fig. 1). The polymer, designated PEP-X, has molecular weight $M = 90\,000$ (polydispersity 1.04), $T_g = -60\,^{\circ}\mathrm{C}$, entanglement molecular weight $M_e \approx 1500$ (i.e., ca. 60 entanglement lengths/chain in the melt), and unperturbed end-to-end dimension $R_0 = 28$ nm. The profiles of normal force F vs the intersurface separation (D) between PEP-X brush-bearing-surfaces across the good solvent cyclohexane (with controls showing the nonadsorbance of PEP alone), Fig. 1, reveal the brushlike nature of the PEP-X layers and their extension L from each surface. They also serve as a systematic control to examine their integrity following shear measurements.

Figure 2 shows characteristic experimental traces of the shear force between the compressed PEP-X-bearing surfaces sliding past each other. The lateral motion Δx_0 applied to the top surface is periodic, consisting of a rest period τ_{rest}, followed by a steady lateral motion at velocity v_s for a further period, and then repeating but with v_s reversed (upper trace, Fig. 2). The lower trace shows the corresponding lateral force $F_s = k\Delta x$ transmitted to the lower surface via the interacting brushes, where k is the stiffness and Δx is the lateral bending of the shear spring S (lower inset, Fig. 1). A number of regimes are clearly indicated (we note that brushes of low T_g end-tethered polyisoprene chains show very similar behavior, not shown here). Initially, as the top surface begins to slide, there is a sharp rise in F_s (regime $a \rightarrow b$ in Fig. 2), during which the surfaces are mostly sliding past each other as the shear force rises. As the layers are highly intertangled when motion begins, this must cause stretching of the chains, as considered below. The maximum in the shear force $F_{s(\max)}$(point b) occurs at a relative sliding of extent 230 ± 20 nm, or some 120 nm per surface; i.e., ca. 20% of the fully stretched end-end dimension L_0 (= 650 nm) of the polymer.

The maximum $F_{s(\max)}$ in the shear force is followed by a slight but marked relaxation, $b \rightarrow c$, and then by subsequent relaxation to a steady state value F_{kin} of the shear force: the kinetic friction at the sliding velocity v_s. Finally, when the applied motion stops, at d, a further relaxation, $d \rightarrow e$, takes place. For the strong compression shown in Fig. 2, the shear force, following an initial rapid

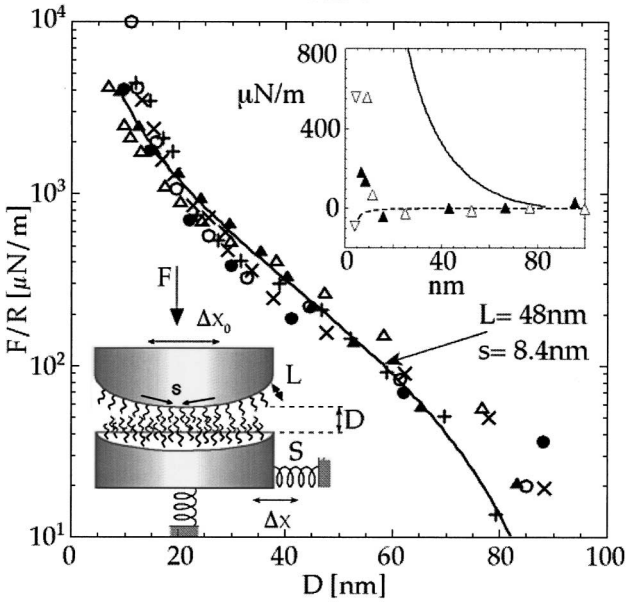

FIG. 1. Force (F/R) vs separation (D) profiles (both approaching and receding), between curved mica sheets (radius R) following attachment from 10^{-4} gm/ml solution of PEP-X molecules in cyclohexane (Merck, Spectroscopic grade). Different symbols are for different runs and experiments, including data (○) taken immediately following a shear measurement. The upper inset shows (F/R) vs D in a 10^{-4} gm/ml solution of unfunctionalized PEP ($M = 290$ K): the absence of any long-ranged repulsion in this case demonstrates that PEP-X attaches to the surface by its zwitterion-terminated end—X only; the solid curve corresponds to the profile with the end-functionalized chains from the main plot. The lower inset illustrates schematically the SFB configuration, with the corresponding structure of the PEP-X brush, where $L_0 = 48 \pm 3$ nm corresponds to half the onset distance for the interaction and the mean interanchor spacing $s = 8.4$ nm is evaluated from adsorbance measurements [14]. The solid curve in the main figure corresponds to the Alexander–de Gennes model [15] with the values of s and L_0 above. Using the Milner-Witten-Cates self-consistent field model [16] with the same s and L_0 parameters gives a similarly good fit to the data.

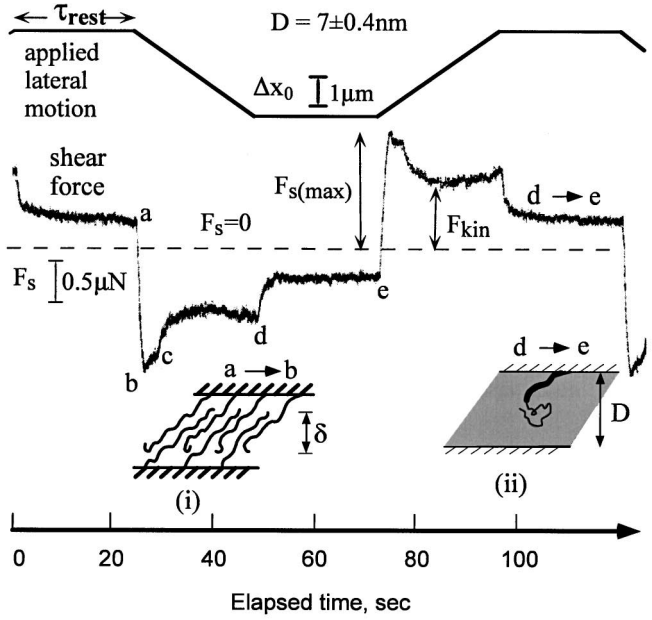

FIG. 2. Shear forces between PEP-X brush-bearing surfaces at separation $D = 7.0 \pm 0.4$ nm. Upper trace: Applied lateral motion (Δx_0) of top mica surface; Lower trace: Shear force F_s transmitted to the lower mica surface. The horizontal broken line represents the midpoint between the shear forces on the back and forth cycles, and is therefore the position of zero shear force when the shear springs are unbent. Inset (i) illustrates the chain configuration in the initial force-rise regime $a \rightarrow b$. Inset (ii) illustrates the relaxation of a chain following cessation of the applied motion at point d (lower trace): the thick part is as yet unrelaxed, while the thin part has relaxed by arm retraction as described in the text.

decay, relaxes only very slowly, and a residual stress is retained across the sheared brushes over the rest periods (of order tens of seconds) in our experiments. Shear force profiles as in Fig. 2 were measured also over a range of different compressions (in the range 5 ± 1 nm $< D <$ 20 nm), shear velocities (in the range 25 nm/s $< v_s <$ 10^4 nm/s) and shear patterns. All cases show the same main qualitative features as in Fig. 2 (though with magnitudes which differed with the parameters): an initial maximum in the shear force $F_{s(\max)}$ which falls to a steady-sliding value F_{kin}, and a subsequent slow decay of the shear force once the applied shear motion ceases.

Figure 3 shows the changes in both $F_{s(\max)}$ and F_{kin} with τ_{rest} prior to sliding, revealing that while $F_{s(\max)}$ rises markedly with τ_{rest}, the kinetic friction is independent of τ_{rest} (an effect noted previously with small-molecule lubricants [17]). Moreover, the kinetic friction (F_{kin}) depends on v_s only very weakly.

These observations shed strong light on the molecular mechanisms underlying the frictional drag between the brush-bearing surfaces. Computer simulation studies [3,9] and self-consistent mean-field models [10,18] suggest that at compressions $D \ll R_0$ the chains should be strongly interpenetrated. In equilibrium (for a gap $D \ll R_0$, as in Fig. 2 where $D = 7$ nm) the end-tethered chains from each surface are then intimately interpenetrated and should be strongly entangled at the high concentrations of the compressed brushes (volume fraction $\phi \approx 0.65$ for the $D = 7$ nm data of Fig. 2). When distorted by shear, their relaxation must therefore proceed by arm retraction, a mechanism similar to that of entangled star-branched chains [7,10,19–21]. A longest relaxation time τ for these tethered chains may be estimated from rheological data on star polymers. For the polymer concentrations and lengths corresponding to the conditions in the present study (e.g., as in Fig. 2), τ is of the order of tens of seconds [22]. The mean shear rate $\dot{\gamma}$ across the gap D, given by $\dot{\gamma} = v_s/D =$ ca. 20 s^{-1} for the conditions of Fig. 2, say, is thus very much greater than the relaxation rate ($1/\tau$), so that the entangled chains must stretch when

their tethered ends begin to move laterally, as adduced for weakly grafted chains sheared by polymer melts or networks [19,20,6]. This is indicated in cartoon (i) in Fig. 2 for the regime $a \rightarrow b$. The force F_s due to this stretching may be evaluated: Since chain elongation is at most some 20% of the fully stretched length, the tension f per chain extended by Δ may be taken as $f \cong 3\Delta k_B T/R_0^2$ [21], yielding $F_s =$ ca. 2.5 μN [23]. Bearing in mind our approximations, the initial observed rise in the frictional drag to $F_{s(\max)} = 1.5$ μN (Fig. 2) is thus accounted for closely by the chain stretching.

At the same time as the elastic tension in the chains increases, they are also being pulled by the sliding motion out of the interpenetration zone [of width δ, Fig. 2(i)], within which they are intertangled with chains from the opposite surface. As a result they experience a weaker drag [20]. The maximum, $F_{s(\max)}$, may be attributed to the point where the increasing chain tension is just balanced by the drag within the interpenetration zone, so that additional tension causes the chains ends to be pulled out faster than the mutual sliding velocity of the surfaces. The chain tension then drops, whereupon chain pullout again slows down. This cascade of relaxations—which results in the regime $b \rightarrow c$ and then finally $c \rightarrow d$ in Fig. 2—is reminiscent of stick-slip behavior in solid friction, though for the brushes it has a very different origin [24], and has been conjectured earlier [7]. The origin of the weak velocity dependence of the kinetic friction F_{kin} (inset to Fig. 3) is probably similar to that for polymer networks sliding past weakly grafted solid surfaces in the so-called marginal regime [5,19,20,6,25]. The analog in the present case of mutually rubbing brushes is that the extent δ of the interpenetration zone in the steady-sliding regime has narrowed to the extent that the relaxation rate of chain moieties within it, $1/\tau(\delta)$, equals (v_s/δ), the shear rate within this zone. At increasing velocity this zone narrows in a self-regulating manner so as to maintain the condition $[1/\tau(\delta)] \cong (v_s/\delta)$, resulting in a frictional drag that varies only very weakly with the sliding velocity, as observed (inset to Fig. 3). The marked increase in $F_{s(\max)}$ with τ_{rest} (Fig. 3), is attributed to the progressive mutual interpenetration of the opposing chain layers during the rest period once sliding stops, leading to greater interpenetration δ at progressively longer τ_{rest}. Once sliding recommences, a correspondingly larger elastic stretching of the interpenetrated chains is then required—manifested as a larger $F_{s(\max)}$—before the tension starts to fall, as described above. The magnitude of F_{kin} for a given v_s, on the other hand, depends only on the stead-state-sliding value of δ, and so is expected to be independent of τ_{rest}, as clearly seen in Fig. 3. An important clue for the relaxation mechanism is revealed on stopping the applied motion, point d in the lower trace of Fig. 2. The form of the relaxation is attributed to the drop in tension in the stretched chains via a chain-retraction mechanism, as theoretically postulated [10,20,21]. The time $t(l_r)$ associated with such a relaxation of a moiety of length l_r varies exponentially with l as $t(l_r) = \tau_1 \exp(\alpha l_r/l_e)$, where τ_1 is a characteristic relaxation time of the relaxed portion l_r of the chain (which varies only as a power of l_r), l_e is the polymer entanglement length, and $\alpha \approx 0.6$ is a constant [26]. The tension $f_s(t)$ in a single chain relaxing by such arm retraction then decays approximately as the remaining unrelaxed portion of the chain, $f_s(t) \propto [L_0 - l_r(t)]$ [21], illustrated in inset (ii) to Fig. 2. From this it is readily shown that $[f_s(0) - f_s(t)]/f_s(0) \cong l_r(t)/L_0 = (l_e/\alpha L_0)\ln[t/\tau_1]$, where $f_s(0)$ is the tension when the chain retraction commences, corresponding in our experiments to the point (d in Fig. 2) at which the applied lateral motion stops, and t is the time over which the relaxation occurs. In terms of the total measured shear force $F_s(t)$ between the surfaces,

$$[F_s(0) - F_s(t)]/F_s(0) \cong l_r(t)/L_0 = (l_e/\alpha L_0)\ln[t/\tau_1]. \quad (1)$$

In Fig. 4 we plot $[F_s(0) - F_s(t)]/F_s(0)$ vs $\ln(t)$ from the shear force trace in the region $d \rightarrow e$. Within the scatter, this indeed yields a straight line (of slope ca. 0.04). The magnitude of the slope $(l_e/\alpha L_0)$ predicted from Eq. (1) is related to the total number $n_e = (L_0/l_e)$ of entanglement lengths in the compressed end-tethered PEP-X brushes, which at the volume fraction ϕ corresponding to $D =$ 7 nm (Fig. 2) is $n_e \approx \phi(M/M_e) \approx 40$; thus $(l_e/\alpha L_0) \approx$ 0.04. In view of our approximations, the closeness of agreement between predicted (ca. 0.04) and experimentally measured (0.038) slopes (Fig. 4) is fortuitous. Nonetheless this quantitative agreement of the magnitude

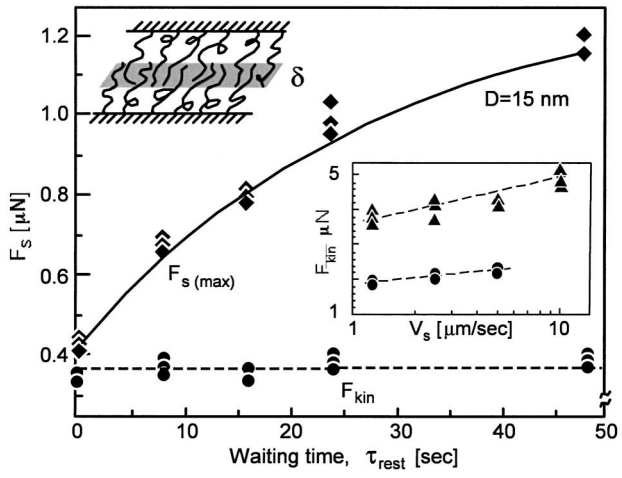

FIG. 3. Variation at $D = 15$ nm of $F_{s(\max)}$ (◆) and F_{kin} (●) with rest period τ_{rest} between shearing cycles (Fig. 2). Inset: Variation of the kinetic friction F_{kin} with sliding velocity v_s at different strong compressions of the PEP-X brushes. (▲): $D = 4.1 \pm 0.4$ nm; ●: $D = 6.2 \pm 0.4$ nm. The cartoon indicates the interpenetration zone, whose width δ increases with increasing waiting time τ_{rest}, but decreases with increased shear velocity v_s (inset), as discussed in the text.

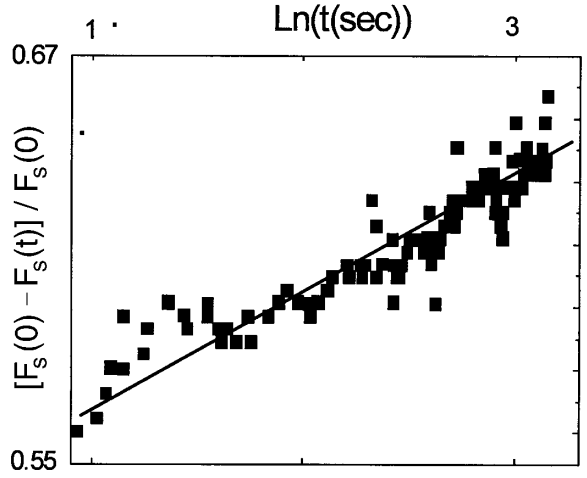

FIG. 4. The relaxation regime for the region marked $d \rightarrow e$ on the right-hand side of the trace in Fig. 2, on an expanded scale, plotted as $[F_s(0) - F_s(t)]/F_s(0)$ vs $\ln[t]$ where $F_s(0) = 0.9\ \mu$N is the value of F_s at the point d; the straight line is a best fit and has a slope 0.038 (see text).

of the slope—with no adjustable parameters—provides strong support (more so than the logarithmic decay alone, which is limited in its dynamic range) for the idea that stress relaxation in the final regime takes place by arm retraction. Such logarithmic surface stress relaxation has not to our knowledge been previously observed. In summary, high-resolution measurement of frictional stresses between polymer brushes sliding past each other shed strong light on the associated molecular mechanisms. They indicate that the initial rise in the frictional drag is due to elastic stretching of the mutually interpenetrated chains, and show that (as chains disengage) this drag falls by a cascade of relaxations to a steady-sliding value characteristic of kinetic friction, whose magnitude is determined by viscous dissipation within a sheared interpenetration zone. On stopping the applied sliding motion, the shear stress across the brushes relaxes logarithmically slowly, consistent with the relaxation by arm retraction of an array of entangled, end-tethered polymer chains.

We thank R. Yerushalmi-Rozen and P. Pincus for critical reading of the manuscript. Financial support of this work by the Israel Science Foundation, the Minerva Foundation, the Deutsches-Israel Program (DIP) and the U.S.-Israel Binational Science Foundation is acknowledged with thanks.

*Present address: Department of Chemical Engineering, Lamar University, P.O. Box 10053, Beaumont, TX 77710, USA.
†Present address: Department of Physics, Jagelonian University, Krakow, Poland.
‡Corresponding author.
Email address: jacob.klein@chem.ox.ac.uk or jacob.klein@weizmann.ac.il
§Present address: Chemical & Biomolecular Engineering, Cornell University, Ithaca, NY 14853, USA.

[1] Z. M. Jin, D. Dowson, and J. Fisher, in *Thin Films in Tribology*, edited by D. Dowson (Elsevier Science Publishers B.V., Amsterdam, 1993).
[2] X. Ma *et al.*, IEEE Trans. Magn. **35**, 2454 (1999).
[3] For a comprehensive recent review emphasizing also simulation work, see G. S. Grest, Adv. Polym. Sci. **138**, 149–182 (1999).
[4] H. R. Brown, V. R. Deline, and P. F. Green, Nature (London) **341**, 221 (1989).
[5] The detailed review by Leger *et al.*, Adv. Polym. Sci. **138**, 185–225 (1999) emphasizes the role of connectors in modifying slip and macroscopic friction [6] at polymer melt and network surfaces.
[6] H. R. Brown, Science **263**, 1411 (1994).
[7] J.-F. Joanny, Langmuir **8**, 989 (1992).
[8] J. Klein, Annu. Rev. Mater. Sci. **26**, 581 (1996).
[9] T. Kreer, M. H. Müser, K. Binder, and J. Klein, Langmuir **17**, 7804 (2001).
[10] T. Witten, L. Leibler, and P. Pincus, Macromolecules **23**, 824 (1990).
[11] P. Schorr, S. M. Kilbey, and M. Tirrell, Polymer Preprints (Abstr. Am. Chem. Soc.) **218: 278-POLY, Pt. 2 AUG**, U477 (1999).
[12] J. Janik, R. Tadmor, and J. Klein, Langmuir **17**, 5476 (2001).
[13] H. J. Taunton *et al.*, Macromolecules **23**, 571 (1990).
[14] R. Tadmor, Ph.D. thesis, Weizmann Institute, 1999.
[15] P. G. de Gennes, Adv. Colloid Interface Sci. **27**, 189 (1987).
[16] S. Milner, T. Witten, and M. Cates, Macromolecules **21**, 2610 (1988).
[17] H. Yoshizawa and J. Israelachvili, J. Phys. Chem. **97**, 11 300 (1993).
[18] C. M. Wijmans, E. B. Zhulina, and G. J. Fleer, Macromolecules **27**, 3238 (1994).
[19] A. Ajdari *et al.*, Physica (Amsterdam) **204A**, 17 (1994).
[20] F. Brochard and P.-G. de Gennes, Langmuir **8**, 3033 (1992).
[21] P. G. de Gennes, *Scaling Concepts in Polymer Physics* (Cornell University Press, Ithaca, New York, 1979).
[22] W. W. Graessley *et al.*, Macromolecules **9**, 127 (1976).
[23] We use the JKR contact mechanics expression for the flattened area $A \approx \pi[RF/K]^{2/3}$, between initially curved surfaces (radius R) with modulus K under a load F, to evaluate the total number (A/s^2) of sheared chains. For a maximal stretching $\Delta = 120$ nm, for which $F_s = F_{s(\max)}$, $F = 40\ \mu$N corresponding to $D = 7$ nm (Fig. 1) and $K = 10^9$ N/m^2 [J. Klein and E. Kumacheva, J. Chem. Phys. **108**, 6996 (1998)], we evaluate the force per surface $F_s = (A/s^2)f$ to be ca. 2.5 μN.
[24] It is of interest that the slight rise in F_s occurs after a time 20 s comparable with the longest relaxations of the tethered PEP chains [22], suggesting that it may be related to more intimate interpenetration following these longest times, though a more detailed consideration is beyond the scope of this Letter.
[25] L. Leger *et al.*, J. Phys. Condens. Matter **9**, 7719 (1997).
[26] See M. Doi and N. Kuzuu, J. Polym. Sci., Polym. Lett. **18**, 775 (1980); J. Klein, Macromolecules **19**, 105 (1986).